Mathematical Theory and Modeling
ISSN 2224-5804 (Paper) ISSN 2225-0522 (Online)
Vol.2, No.10, 2012

An algorithm for simulation of a Chemical Transport Equation in an Aquifer

Enock Okiambe [1, 2]*, Willis Ambusso [1], Benson Ng'ang'a [1] and Richard Mogwasi [2]

1. Department of Physics, Kenyatta University, P.O Box 43844 Nairobi, Kenya
2. Department of Applied Sciences, Gusii Institute of Technology, P.O Box 222, Kisii, Kenya

* E-mail of the corresponding author: enockokiambe@gmail.com

Abstract

Dynamical systems can be predicted using mathematical models. These models are usually Partial Different Equations (PDEs). Examples include the wave equation, equations for diffusive processes, and the heat conduction equation. Numerical solution of such PDEs describing a given system and its implementation using a suitable computer code can lead to numerous predictions on the dynamical system both in space and time. In this paper, the contaminant / chemical equation and the groundwater flow equation are solved numerically using the Integrated Finite Difference Method (IFDM) and the algorithms generated are simulated using an object oriented code. Generic results generated represent important predications on the fate and transport processes of a chemical in an aquifer

Keywords: Simulation procedure, integrated finite difference method, contaminant equation, discretization

1. Introduction

Groundwater reservoirs are used for both household purposes and for commercial purposes e.g. irrigation. Contamination of these resources by nutrients especially in agricultural watersheds should be monitored. For example, nitrogenous fertilizers which are highly used as plant growth enhancers, leaches to groundwater in the form of nitrate which are highly mobile and suffer little sorption. This takes place when the fertilizer application exceeds the plant demand and the denitrification capacity of the soil (Meisinger & Randall, 1991; Birkinshaw & Ewen, 2000; Shamrukh *et al.*, 2001). Once in the groundwater, nitrate can accumulate to undesirable levels causing deterioration of groundwater quality. Studies have shown that, the use of groundwater-based drinking water supplies with nitrate concentrations exceeding a Maximum Contamination Level (MCL) of 45mg/l NO_3^- (US EPA,1995), can cause methemoglobinemia in infants and stomach cancer in adults (Lee *et al.*, 1991; Wolfe & Patz, 2002). More recent studies have indicated positive correlation between nitrate exposure levels and both bladder and ovarian cancer in women (Weyer & Cerhan, 2001).

Nitrate like other solutes in groundwater, interacts with the fluid and solid phases of the porous media through a variety of processes. These include; chemical diffusion, mechanical dispersion, advection, chemical reaction, sorption, and decay. These processes are all involved in the chemical equation. The withdrawal of water containing the contaminant from the aquifer through a well or injection of such water into it (sources and sinks) appear in the chemical transport equation as a boundary condition. The solution of this equation readily makes it possible to predict contamination extents in aquifers. Many times, field measurements to determine contamination levels, are expensive to carry out, partly because of the relative inaccessibility of the aquifers and the high expenses involved in performing the actual field experiments.

2. The Governing Equations

The partial differential equation governing the 3- D transport of a single chemical constituent in an aquifer, considering transport processes, fluid sources and sinks, sorption, and first order irreversible rate reactions is given as follows (Zheng & Bennett,1995) ;

$$R\frac{\partial C}{\partial t}=\frac{\partial}{\partial x_i}\left(D_{ij}\frac{\partial C}{\partial x_j}\right)-\frac{\partial}{\partial x_i}\left(v_i C\right)+\frac{q_S}{\theta}C_S-\lambda\left(C+\frac{\rho_b}{\theta}\overline{C}\right) \quad (1)$$

Where C is the dissolved concentration (ML^{-3}); $\overline{C}$ is the adsorbed concentration (MM^{-1}); t is time (T); D_{ij} is the hydrodynamic dispersion coefficient tensor (L^2T^{-1}); v_i is the pore water velocity (LT^{-1}); q_s is the volumetric flow rate per unit volume of aquifer-representing fluid sources and sinks (T^{-1}); C_s is the concentration of the fluid source or sink flux (ML^{-3}); λ is the reaction rate constant (T^{-1}); R is the retardation factor (L^0); ρ_b is the bulk density of the porous medium (ML^{-3}); $x_{i,j}$ is the distance along the respective Cartesian coordinate axis (L); and θ is the porosity (L^0).

$$R=\frac{v'}{v_s} \quad (2)$$

Where v' is the average linear velocity of the groundwater and v_s the linear velocity of the retarded constituent. It follows from equation (2) that for a retarded chemical, R must be greater than one. For chemicals that do not adsorb, e.g. nitrate, the retardation coefficient is assumed to be 1. In such case, equation (1) reduces to;

$$\frac{\partial C}{\partial t}=\frac{\partial}{\partial x_i}\left(D_{ij}\frac{\partial C}{\partial x_j}\right)-\frac{\partial}{\partial x_i}\left(v_i C\right)+\frac{q_S}{\theta}C_S-\lambda C \quad (3)$$

Equation (4) for the 3-D groundwater flow model is solved to obtain the head distribution and subsequently the velocity field for use in equation (3) to account for advection transport of the chemical (Schwartz & Zhang, 2003).

$$\frac{\partial}{\partial x}\left(K_{xx}\frac{\partial h}{\partial x}\right)+\frac{\partial}{\partial y}\left(K_{yy}\frac{\partial h}{\partial y}\right)+\frac{\partial}{\partial z}\left(K_{zz}\frac{\partial h}{\partial z}\right)-W=S_s\frac{\partial h}{\partial t} \quad (4)$$

Where K_{xx}, K_{yy} and K_{zz} are values of hydraulic conductivity along x-, y-, and z- coordinate axes (LT^{-1}); h is the hydraulic head (L), W is a flux term that accounts for pumping, recharge, or other sources and sinks (T^{-1}); S_s is the specific storage (L^{-1}); t is time (T).

Velocities are computed from equation (4) using the Darcy equation;

$$v=K\frac{\partial h}{\partial x} \quad (5)$$

2.1 Discretization of the Governing Equations

Discretization is the process of breaking the governing equations into discrete components that can be implemented using computer codes; making it possible for an equation to correspond to each cell in the discretised aquifer. This is done because usually reservoirs are heterogeneous i.e., the hydraulic properties vary from point to point within the aquifer.

The Partial Differential Equations above are discretised using the IFDM. In this method, nodes are centered in the middle of the blocks and flows are assumed to occur perpendicularly to the boundaries of the blocks. Flows between nodes can then be computed using Darcy's law and the head gradient defined as the difference in heads between neighboring nodes. With this assumption, a system of equations is constructed with one equation for each node. This makes it possible to apply Gauss divergence theorem to the governing equations, converting the integration over block volume to block faces. This method of solution for the model equations is elaborated as follows;

Equation (4), when written in indicial form reduces to;

$$\frac{\partial}{\partial x_i}\left(k_{i,j}\frac{\partial h}{\partial x_j}\right)-W=S_s\frac{\partial h}{\partial t} \qquad (6)$$

Where *i, j* = *x, y* or *z* for three dimensional flow

Since hydraulic properties are averaged for each block volume, equation (6) can be integrated over the entire block volume V, to yield;

$$\int_V \frac{\partial}{\partial x_i}\left(k_{i,j}\frac{\partial h}{\partial x_j}\right)dV-W_V=\int_V S_s\frac{\partial h}{\partial t}dV \qquad (7)$$

Applying Gauss's Divergence theorem on the term containing the space coordinates in (7) makes it possible to move from volume integral to surface integral. This reduces the order of the PDE by one to a first order and it becomes;

$$\int_s k_{i,j}\frac{\partial h}{\partial x_j}ds_{i,j}-W_V=VS_s\frac{\partial h}{\partial t} \qquad (8)$$

Integration over the entire system surface is equivalent to summing over individual block surfaces where interaction with respective neighbors does takes place and then again summing over all the blocks in the aquifer system. Equation (8) the becomes;

$$\sum k_{i,j}\frac{\partial h}{\partial x_{i,j}}ds_{i,j}-W_V=VS_s\frac{\partial h}{\partial t} \qquad (9)$$

Equation (10) represents the discretised form of equation (9) which is an algorithm for use in a computer program. It is expressed in the fully explicit form which uses the present parameter values in calculating the new values in the next time step. It is relatively easy to code an algorithm expressed in the explicit form,

$$\sum k_{i,j}\frac{\left(h_j^{\,t}-h_i^{\,t}\right)}{\Delta x_{i,j}}\Delta s_{i,j}-W_V=VS_s\frac{\left(h_i^{\,t+1}-h_i^{\,t}\right)}{\Delta t} \qquad (10)$$

This can further be rearranged as follows;

$$h_i^{\,t+1}=h_i^{\,t}\left(1-\frac{\Delta t}{VS_s}\sum k_{i,j}\frac{\Delta s_{i,j}}{\Delta x_{i,j}}\right)+\frac{\Delta t}{VS_s}\sum k_{i,j}\frac{\Delta s_{i,j}}{\Delta x_{i,j}}h_j^{\,t}-\frac{\Delta t}{VS_s}W_V \qquad (11)$$

Where $h_i^{\,t+1}$ and $h_i^{\,t}$ are the head value for the next time step and for the present time step respectively for block *i*, being the block under consideration with its neighboring blocks, *j*. Considering each block, equation (11) yields a system of algebraic linear equations whose solution results into the field head distribution pattern for the water system under study.

The chemical equation given in (3) is integrated over block volume to yield;

$$\int_V \frac{\partial C}{\partial t}dV=\int_V \frac{\partial}{\partial x_i}\left(D_{i,j}\frac{\partial C}{\partial x_j}\right)dV-\int_V \frac{\partial}{\partial x_i}\left(v_i C\right)dV+\frac{q_s C_s}{\theta}-\lambda C \qquad (12)$$

Following similar approach used for discretization of (4), the final algorithm for (12) becomes;

$$C_i^{t+1} = C_i^t \left(1 - \frac{\Delta t}{V}\sum D_{i,j}\frac{\Delta s_{i,j}}{\Delta x_{i,j}}\right) + \frac{\Delta t}{V}\sum D_{i,j}\frac{\Delta s_{i,j}}{\Delta x_{i,j}} C_j^{\,t} - \frac{\Delta t}{V}\sum v_i C_i ds_{i,j} + \frac{\Delta t}{V}\left(\frac{q_s C_s}{\theta} - \lambda C_i\right) \quad (13)$$

The v_i in equation (13) is calculated from equation (11) using the Darcy equation. Its discretised form is follows;

$$v_i = \sum k_{i,j}\frac{\left(h_j^{\,t} - h_i^{\,t}\right)}{\Delta x_{i,j}} \quad (14)$$

2.2 Aquifer discretization

For the algorithms to apply to an aquifer domain, the continuous aquifer domain is replaced by a discretised domain, which consists of an array of nodes and associated finite difference blocks or cells (Anderson & Woessner, 1992). A node represents a single point on each cell at which the hydraulic property is averaged or calculated. The size of the node is determined by the extent to which hydraulic properties vary throughout the modeled area.

Figure 1 shows a cell *i* on a single grid layer with its neighbors A, B on one direction and C, D on the other. For a Cartesian grid, the directions are defined as in figure 2. The longitudinal direction coincides with the principal direction of flow of water.

3. Results and discussions

A computer code was written to solve the algorithms obtained over a two layered rectangular grid system. The following generic tests were done and predictions made.

3.1 Hydraulic Head Distribution Levels

The results obtained by the simulator due to pumping and injection tests (on block 0), are as given in figure 3 and 4. The results are in agreement with the laws governing groundwater flow. As expected the characteristic pattern of the head distribution curve during pumping is such that the level first goes down according to the characteristic shape of the transient region and later the piezometric surface no longer changes much; the aquifer goes down uniformly; its evolution at one point is coupled with its evolution at all other points and the drawdown velocity is uniform.

3.2. Effects of Transport Processes and Decay on Chemical Concentration Curves

Tests were done to investigate how each of the transport processes affected the concentration of the chemical at any given time after its instantaneous injection at a point in the aquifer. The modular approach of the object-oriented programming language makes this possible. Figure 5 shows the concentration breakthrough curves for advection transport only. It shows that the concentration available to the next neighboring point reduces with distance from the injection point, indicating that dilution is taking place. Consequently the concentration level in the source point reduces as the chemical is passed to the neighborhood.

Figure 6 compares the concentration curves for the two transport processes. The concentration peak value for the dispersion curve is far higher than that of advection, meaning that the chemical takes a long time to reach neighboring horizons and so a longer retention time. Also using an up-scaled value for the decay constant of 4.0 d^{-1}, the simulator was capable of indicating the effect of decay in the cell in the presence of advection (figure 7). In such case it is observed that the chemical concentration decreases in the presence of denitrification.

3.3. Effect of Hydraulic Properties on the Chemical Concentration

The influences of the two key field quantities that relate to chemical concentration were examined. They involve porosity and dispersion coefficient. How the concentration changes with respect to changes in grid size was also investigated.

The result in the figure 8 indicates that the diffusivity value varies directly with the concentration peak values but peak arrival time shows an inverse relation. This is expected because a high value of diffusivity means that the solute diffuses through the entire grid volume much faster than otherwise. Hence at high values it will do so a little quickly leading to a higher concentration value before being transported out of the cell through advection process. The transport out of the grid cell takes a longer time in the case of lower diffusivity. This is the reason for a weak peak for small values of diffusivity implying that the solute is slowly given out from one block to another. However in effect, dispersion proves to be a weak process of solute transport relying mainly on big value differences for any noticeable change on the profiles.

Porosity is defined as the ratio of voids to the total volume of a porous media sample. A higher porosity percentage would mean more volume to receive a given concentration of a chemical being injected into a grid cell as opposed to a relatively lower percentage. In a given time interval the concentration will be expected to vary inversely with the porosity value. This is what is shown in figure 9. Peak arrival time remains nearly the same for all porosity values because once injected into a grid cell, the chemical has to interact with all the water molecules in a given control volume before being passed to neighboring cells.

Changing the grid size by a factor of 4, affects the concentration significantly (figure 10). At higher grid sizes, the concentration peak is far lower than for smaller grid sizes. This is physically expected because the solute is now interacting with more fluid particles than before. In a way, the ratio of the solute particles to fluid particles is increased in case of lower grid sizes.

4. Conclusions

The sensitivity of the model to indicate the effect of various aquifer characteristics on the head and concentration profiles proves the success of the simulation procedure i.e. the solution of the governing equations and their coding. In general the results generated at generic testing using the simulator were physically reasonable and feasible. This means that the simulator can be used in field simulation to predict and monitor chemical behavior once introduced into the aquifer.

References

Anderson, M.P. and Woessner, W.W. (1992), Applied groundwater modeling: simulation of flow and advective transport. Academic Press, San Diego, pp 13.

Birkinshaw, S.J. and Ewen, J. (2000), Nitrogen transformation component for SHETRAN catchment nitrate transport modeling. *Journal of Hydrology* 230.

Lee, Y.W., Dahab, M.F. and Bogardi, I. (1991), Nitrate risk management under uncertainty. *Journal of Water Resources Planning and Management* 118 (2): 151.

Meisinger, J.J. and Randall, G.W. (1991), Estimating N budgets for soil crop systems. In: Follet, R.F., Keeney, D.R., Cruse, R.M. (Eds.), Managing N for Groundwater Quality and Farm Profitability. Soil Society of America, Madson Wisconsin, pp. 85.

Schwartz, F. and Zhang, H. (2003), Fundamentals of Groundwater. John Wiley and Sons, Newyork. Pp 206-276.

Shamrukh, M., Corapcioglu, M. and Hassona, F. (2001), Modeling the effect of chemical fertilizers on groundwater quality in the Nile Valley Aquifer, Egypt. *Ground Water* 39(1): 59.

U.S. Environmental Protection Agency. (1995), Drinking Water Regulations and Health Advisories. Office of Water, Washington, DC.USA.

Weyer, P.J. and Cerhan, J.R. (Eds.). (2001), Municipal drinking water nitrate level and cancer risk in older women:

the Iowa women's study. *Epidemiology* 11 (3): 327.

Wolfe, A.H. and Patz, J. A. (2002), Reactive nitrogen and human health: acute and long-term implications. Ambio 31(2), 120.

Zheng, C. and Bennett, G.D, Applied Contaminant Transport Modeling: Theory and practice. Van Nostrand Reinhold, New York, 440pp, 1995.

Figures

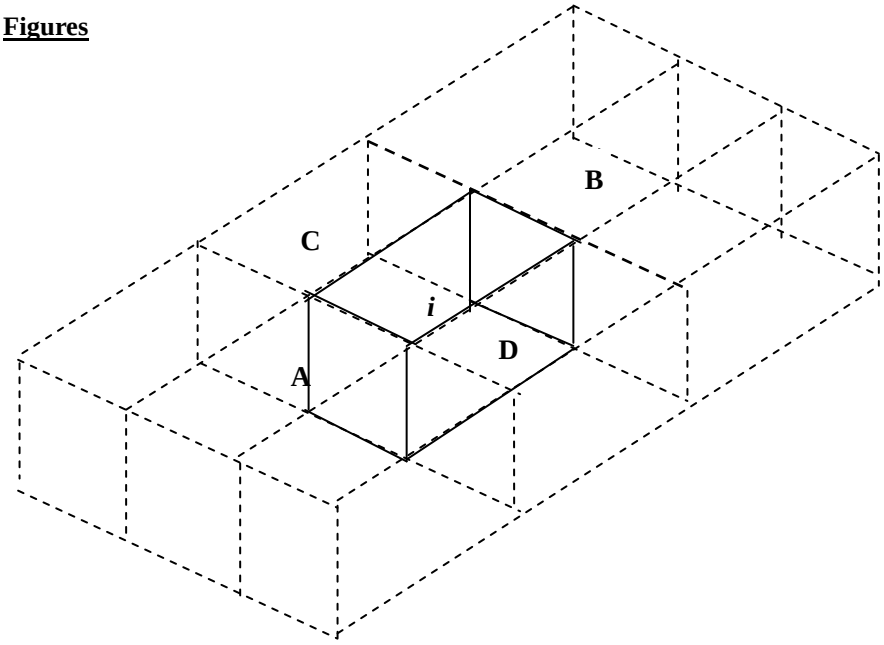

Figure 1: Mesh showing a block *i* and its neighbors

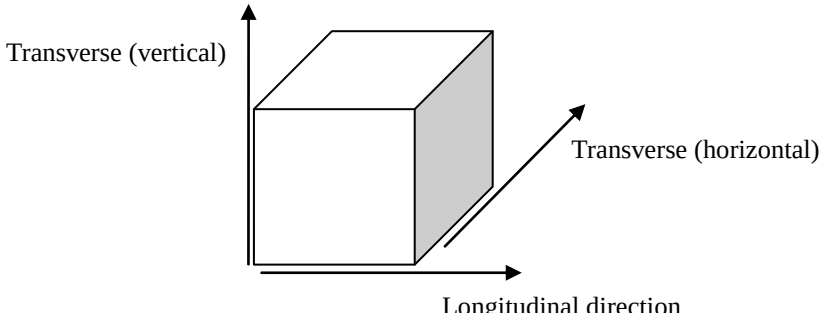

2. Defining the grid directions

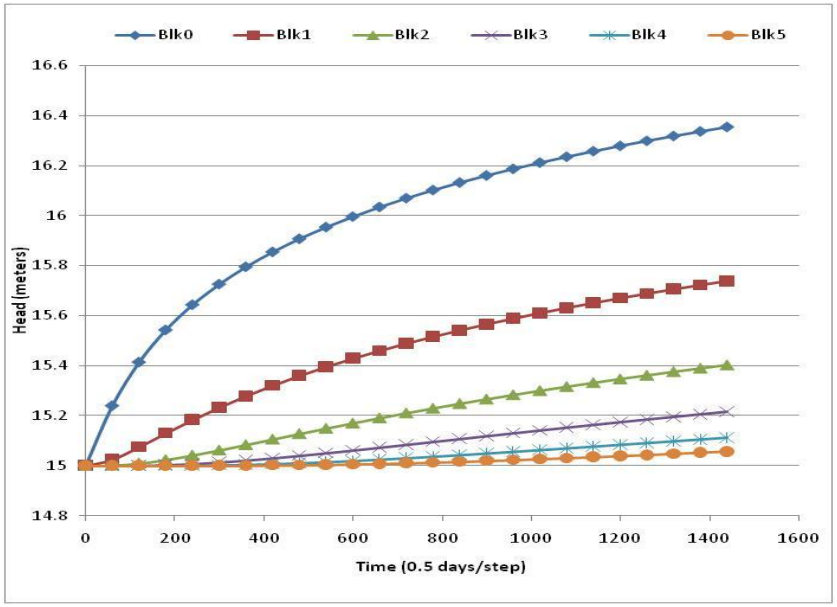

Figure 3: Head distribution due to continuous injection at a point source (block 0)- blocks 1,…..5 follow each other consecutively from the injection block.

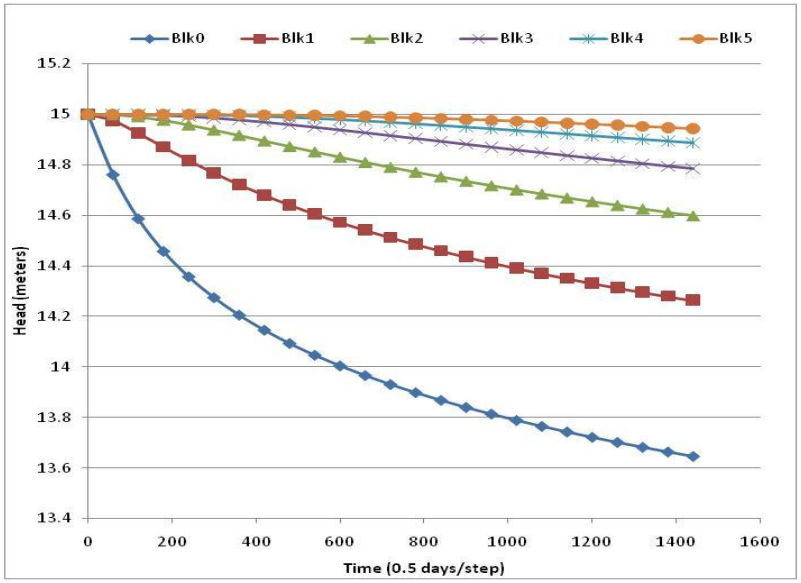

Figure 4: Head distribution due to continuous pumping rate

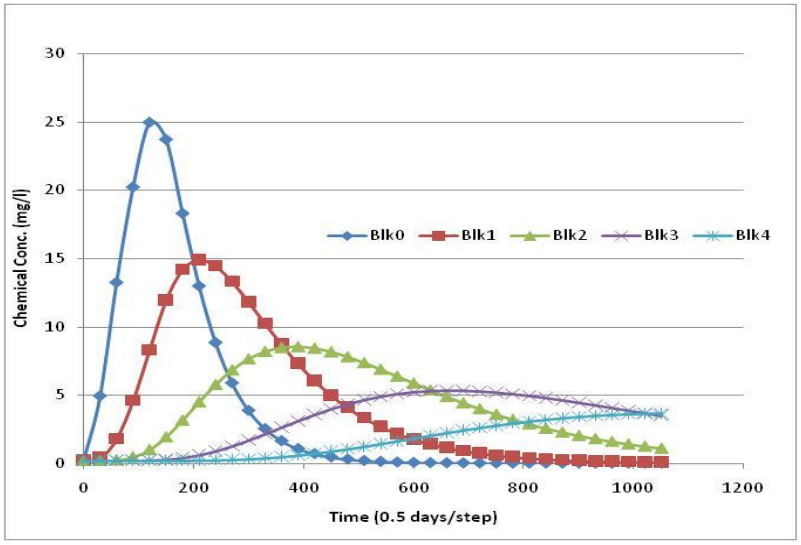

Figure 5: Breakthrough curve for temporal chemical concentration due to advection transport

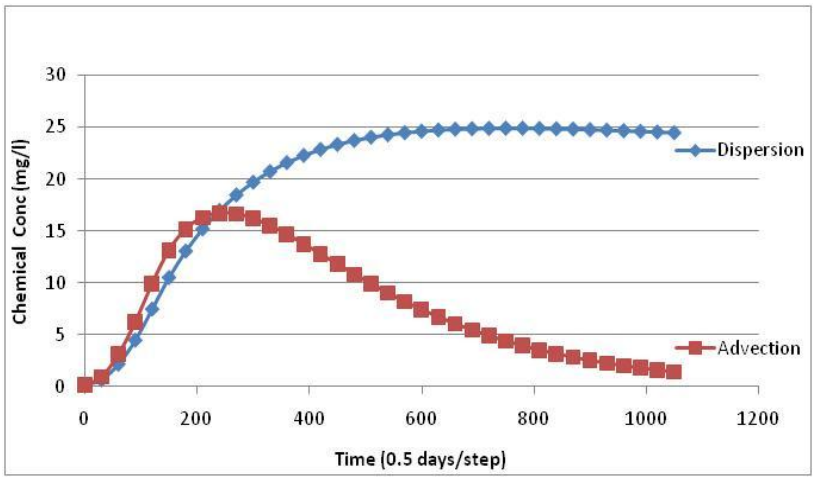

Figure 6: Comparison of advection and dispersion transport processes

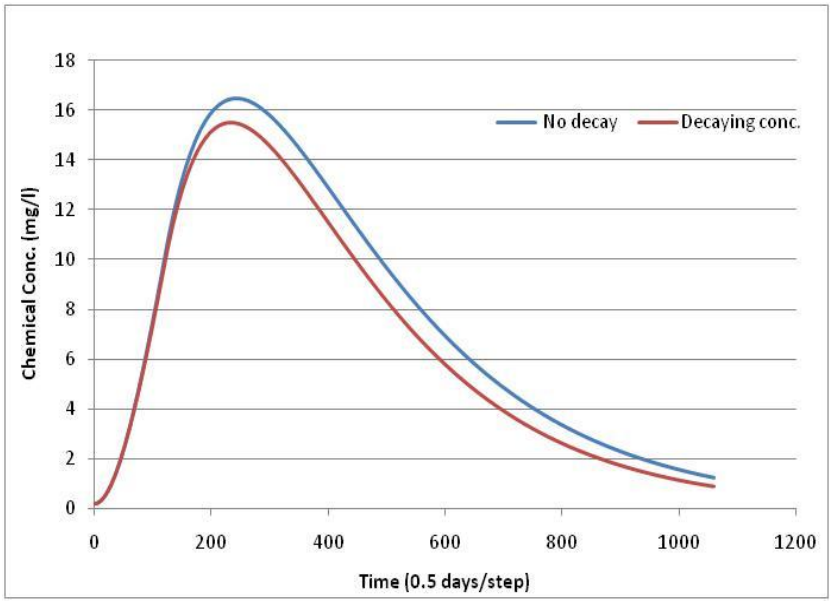

Figure 7: The effect of denitrification on the temporal nitrate concentration level

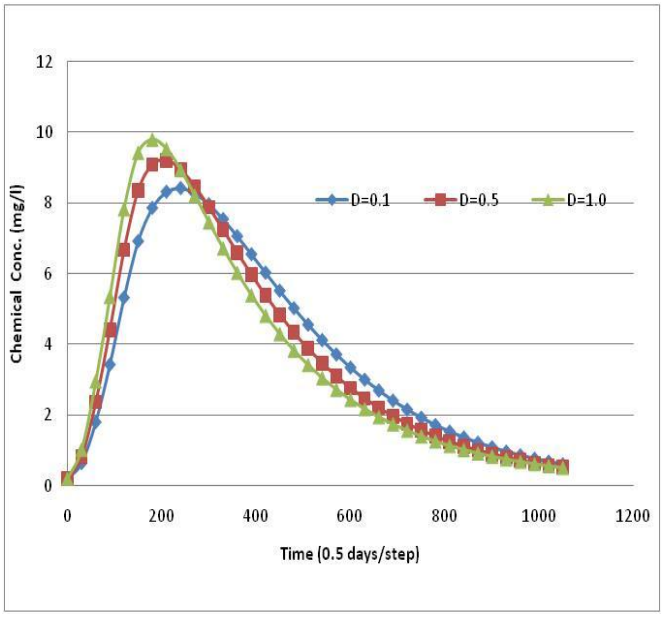

Figure 8: The influence of dispersion coefficient on nitrate concentration level.

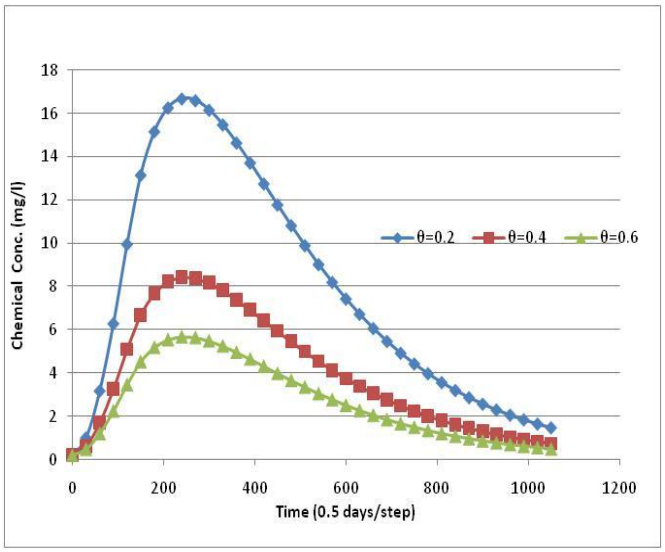

Figure 9: Variation in nitrate concentration levels for different porosities.

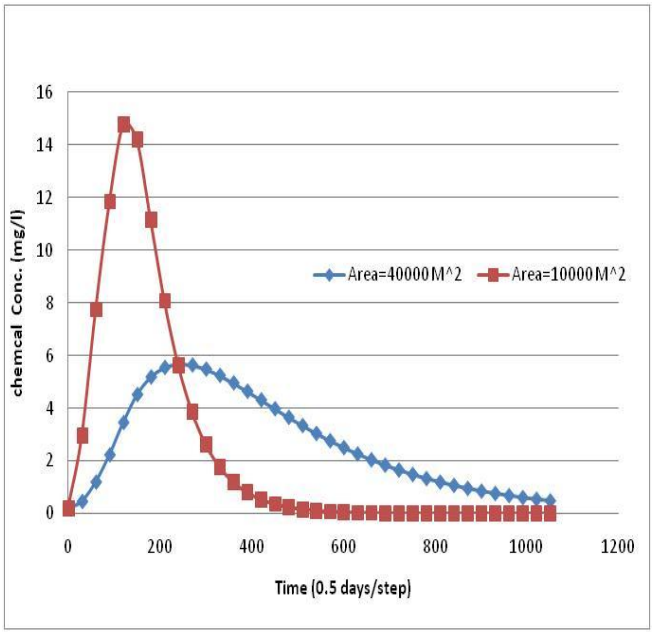

Figure 10: Effect of change of the grid size on the nitrate concentration profiles

This academic article was published by The International Institute for Science, Technology and Education (IISTE). The IISTE is a pioneer in the Open Access Publishing service based in the U.S. and Europe. The aim of the institute is Accelerating Global Knowledge Sharing.

More information about the publisher can be found in the IISTE's homepage: http://www.iiste.org

CALL FOR PAPERS

The IISTE is currently hosting more than 30 peer-reviewed academic journals and collaborating with academic institutions around the world. There's no deadline for submission. **Prospective authors of IISTE journals can find the submission instruction on the following page:** http://www.iiste.org/Journals/

The IISTE editorial team promises to the review and publish all the qualified submissions in a **fast** manner. All the journals articles are available online to the readers all over the world without financial, legal, or technical barriers other than those inseparable from gaining access to the internet itself. Printed version of the journals is also available upon request of readers and authors.

IISTE Knowledge Sharing Partners

EBSCO, Index Copernicus, Ulrich's Periodicals Directory, JournalTOCS, PKP Open Archives Harvester, Bielefeld Academic Search Engine, Elektronische Zeitschriftenbibliothek EZB, Open J-Gate, OCLC WorldCat, Universe Digtial Library , NewJour, Google Scholar